Discrete Periodic Radon Transform based Weighted Nuclear Norm Minimization for Image Denoising

Budianto and Daniel P.K. Lun*
Centre for Signal Processing, EIE
Department of Electronic and Information Engineering
The Hong Kong Polytechnic University
Hong Kong
*enpklun@polyu.edu.hk

***Abstract*— A novel image denoising scheme based on the weighted nuclear norm minimization (WNNM) is proposed. For effective denoising of natural lines/edges with prominent singularities, the WNNM operator is applied in the discrete periodic Radom transform (DPRT) domain. With a careful examination of the statistic of DPRT coefficient, we can decompose the image patches into two parts, the strong edges patches and the smooth patches. For patches with edges, the WNNM operator is performed in DPRT domain which is also an invertible transform with a perfect reconstruction property. For the smooth patches, the conventional WNNM operator is performed in the spatial domain. Simulation results unto the various testing images shows that our approach achieves a substantial improvement in term of both peak signal-to-noise (PSNR) ratio and in visual quality as compared with other state-of-the-art image denoising approach.**

Keywords*— *Image denoising, group-based denoising, weigted nuclear norm minimization (WNNM), discrete periodic Radon transform (DPRT), BM3D.

I. INTRODUCTION

As a fundamental problem in image processing, image denoising methods have been around for decades but still have room for further improvement, as mentioned in [1]. In the last decades, the major improvement in image denoising is obtained by exploiting the similarity among neighboring patches. It was first pioneered in [2] which employs a nonlocal self-similarity as its main procedure. It can be performed either in the spatial domain as in [2] or in the transform domain as in [3, 4]. In [3], an enhancement of the sparsity in transform domain can be achieved by grouping similar 2D patches and applying 2-steps denoising procedure using wavelet transform and Wiener filter.

Recently, a low-rank reconstruction is proposed. The idea is to learn dictionaries for image denoising using low rank approximation in term of the singular value decomposition (SVD) of a set of training image-patches[5]. Although it is simple and efficient, its performance is rather low since it ignores the relationship between similar patches nearby. Applying the low rank minimization approach to a matrix of similar patches has been proved to achieve highly competitive denoising results [6, 7]. In [7], a weighted nuclear norm proximal (WNNM) operator aiming to recover the low rank matrix of similar patches of its noisy observation is investigated. However, it considers only similar patches based on the Euclidian distance but ignoring the structure of the similar patches. As an improvement of [7], [6] introduces pre-filtering strategy using existing denoising algorithm, i.e., block matching and 3D filtering (BM3D) [3]. Then the residual of the denoised image is fed back to the denoising procedure to further improve its performance. Albeit its success as aforementioned, low rank image denoising still has certain limitations. For instance, all patches within the same group are treated with the same strategy in the spatial domain. Hence, it might not be optimum when applying to the sharp edges which can have significant differences in the spatial domain.

In this paper, we propose a new image denoising scheme based on WNNM [6]. To improve the denoising performance, the discrete periodic radon transform (DPRT) is employed. The DPRT is the discrete version of the traditional Radon transform, but has a perfect reconstruction method. Furthermore, the nuclear norm regularization in the DPRT domain perfectly fits to the natural lines/edges with prominent singularities. It allows them to be effectively denoised. However, it is crucial for DPRT-based denoising exhibits different properties which must be considered when we seek to an effective denoising. For the strong projection of DPRT corresponding to natural edges to be denoised, they will provide a point singularity when they are mapped onto the DPRT domain. A nuclear norm regularization in the DPRT domain can be performed for these strong projections to achieve an effective denoising performance. For the smooth region, the nuclear norm regularization is performed in the spatial domain as in the conventional WNNM approach. It is to avoid "wrap around" effect which disperses the energy distribution in the DPRT domain[8]. Note that to classify the edges and smooth area, we use the statistic of the DPRT coefficients. Experimental results show that the proposed technique can significantly improve the denoising performance outperforming the state of the art denoising method such as BM3D, multi-scale patch-based image restoration (MSEPLL), WNNM, and group sparsity residual constraint (GSRC). An overview of the proposed denoising framework is shown in Fig. 1. First, the background of DPRT and WNNM will be laid out in Section II and our proposed denoising algorithm will be explained in more detail in Section III.

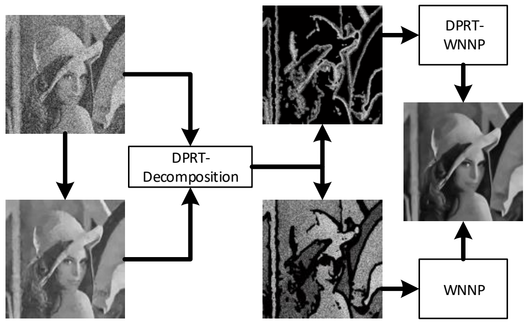

Fig. 1. The overview of the proposed denoising framework

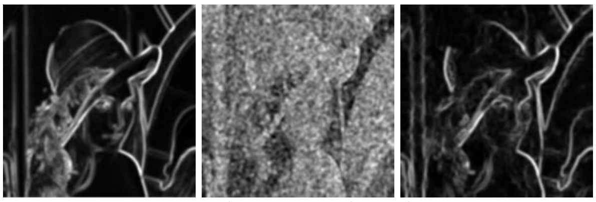

Fig. 2. The sampling points of Fourier transform of C_2 and C_3 on the original discrete patch spectrum (a patch of size 7×7);

II. DPRT

In short, DPRT can be considered as a prime case of discreet Radon transform which preserves most of the important properties of the continuous Radon transform. Assume a set of integers as $\{0,1,2,\ldots,\mathrm{n}-1\} \subset \mathbb{Z}$ as $\mathbb{Z}_n$, $\mathbb{Z}_n \times \mathbb{Z}_n$ as $\mathbb{Z}_n^2$. Denote that $l^2(\mathbb{Z}_n^2)$ to be a set of doubly summable 2D function over $\mathbb{Z}^2$. Given a patch $f \in l^2(\mathbb{Z}_p^2)$ in the case that p is prime, its DPRT transform can be defined as follows,

$$C_m(d) = \sum_{x=0}^{p-1} f(x, \langle d + mx \rangle_p)$$
$$B_0(d) = \sum_{x=0}^{p-1} f(d, y) \quad (1)$$

where $m, d \in \mathbb{Z}_\mathrm{p}$ and $\langle a \rangle_p$ is the modulo of an integer a by a positive integer p. (1) shows that all DPRT projections of a patch are simple summation operations taken from different angles m in a periodic faction.

DPRT also have a relationship known as the discreet Fourier slice theorem. Suppose the original spectrum of a patch f is

$$\mathcal{F}(u, v) = \sum_{x=0}^{p-1}\sum_{y=0}^{p-1} f(x, y) e^{-j2\pi(ux+vy)/p} \quad (2)$$

where $u, v \in \mathbb{Z}_p^2$. The spectrum in (2) is related to the spectrum of its DPRT projections as follows:

$$\mathcal{F}(\langle -mv \rangle_p, v) = \sum_{y=0}^{p-1} c_m(d) e^{-j2\pi(vd)/p}$$
$$\mathcal{F}(u, 0) = \sum_{y=0}^{p-1} b_0(d) e^{-j2\pi(ud)/p} \quad (3)$$

This states that the Fourier transform of a DPRT projection is the same as one slice of the original discrete 2D spectrum as seen

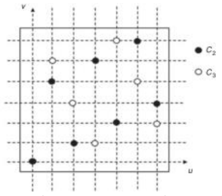

Fig. 3. The sampling points of Fourier transform of C_2 and C_3 on the original discrete patch spectrum (a patch of size 7×7);

in Fig. 3. The DPRT is also an invertible transform which has a perfect reconstruction property.

III. DPRT ASSISTED WNNM

Let us first assume that $F^n \in \mathbb{R}^{m \times n}$ be a noisy observation image matrix. The image denoising aims to estimate the original image F from the noisy observation which can be written as,

$$F^n = F + N, \quad (4)$$

where N is a Gaussian noise with zero means and variance σ_n^2 .

Using the property of non-local similarity structures of an image, recent works [3, 7, 9] have shown a powerful image denoising performance. In these approaches, an image F is divided into n overlapped patches f_i of size $\sqrt{bc} \times \sqrt{bc}$, $i = 1, \ldots, n$. Then for each local patch f_i of image F, we find its similar k patches in the an $L \times L$ search windows. This set of similar k patches than is vectorized and stacked into each column of a matrix $F_i \in \mathbb{R}^{bc \times k}$ where each column corresponding to each patch. Hence the matrix F_i contain all patches with similar structures called group. Using weighted nuclear norm proximal (WNNM) operator, matrix F_i then can be estimated by solving [7],

$$\hat{F}_i = argmin_{X_i} \|F_i^n - F_i\|_F^2 + \lambda \|F_i\|_*. \quad (5)$$

(5) has closed-form solution by applying a soft-thresholding operation to the singular value of the observation matrix F_i^n from the noisy patches, $\hat{F}_i = US_{\lambda/2}(\Sigma)V^T$, where $S_\lambda(\Sigma) = \max(\Sigma_{ii} - \frac{\lambda}{2}, 0)$ and $F_i^n = \mathrm{U\Sigma V^T}$. In [7], Gu *et all.* Introduces the weight vector to improve (5) such that the problem in (5) has a close form solution as

$$\hat{F}_i = U\hat{\Sigma}V^T. \quad (6)$$

The diagonal element $\hat{\Sigma}$, $diag(\hat{\Sigma}) = \sigma_1(\hat{X}_i), \sigma_2(\hat{X}_i), \ldots, \sigma_n(\hat{X}_i)$ can be estimated by,

$$\sigma_i(\hat{X}_i) = \begin{cases} 0 & if\ c_2 < 0 \\ \dfrac{c_1 + \sqrt{c_2}}{2} & if\ c_2 \geq 0 \end{cases} \quad (7)$$

where $\mathrm{c}_1 = \sigma_i(Y) - \varepsilon$,

$$\mathrm{c}_2 = (\sigma_i(Y) + \varepsilon)^2 - 4C \quad (8)$$

and $\mathrm{C} = \sqrt{2n}$ with n is the number of similar patches.

In conventional WNNM, the denoising algorithm is solved by applying the above solution to all patches iteratively. In each iteration, first each group patches selected from a noisy image are denoised using WNNM operator. Finally, the resulting patches are aggregated back to form the clean image. Although it is simple and effective, it employs only non-local similarity property of the noisy image in the spatial domain. Hence it might not be optimal to all various groups of patches, especially those with strong edges.

Intuitively, one can perform the WNNM operator in the DPRT domain to take its advantages by mapping the linear singularities, i.e., edges, in the spatial domain into several DPRT projections. While it is easy to perform, it might not be optimum since, as shown in (1), DPRT domain is a set of discreet line summations of pixels. To accommodate this summations in the nuclear norm estimation, c_2 in (8) can be rewritten as follows,

$$c_2 = (\sigma_i(Y) + \varepsilon)^2 - 4pC \qquad (9)$$

where p is the patch size and is a prime. Note that (9) will not give any significant improvement in the denoising performance. It is due to the "wrap around" effect of the DPRT domain. Since an image consists of both smooth and edges region, DPRT domain will only improve in the edges area but not the non-edges area. Hence there needs to be an effective process to decompose the edges and non-edges. While it is tempted to have another effective decomposition algorithm, we can employ the statistic of DPRT for free. As mentioned above, DPRT can maps the linear singularities of the spatial domain into several projections in the DPRT domain. Take λ as a the threshold to distinguish the edges and non-edges patches, WNNM operator is applied to the spatial domain for non-edges patches and to DPRT domain for edges patches, such that c_2 can be estimated as follows

$$c_2 = \begin{cases} (\sigma_i(Y) + \varepsilon)^2 - 4C, & E > \lambda \\ (\sigma_i(Y) + \varepsilon)^2 - 4pC & E \le \lambda \end{cases} \qquad (10)$$

where $\mathrm{E} = \mathrm{std}(\mathcal{F})$, the standard deviation of the DPRT coefficients in (2) for a given patch $f \in l^2(\mathbb{Z}_p^2)$. By experience, we set $\lambda = 20$. The visualization in spatial domain of the decomposition can be seen in Fig. 4. Fig. 4 (left) shows the aggregated image obtained using (10)with the patch size of 7×7. As shown in the figure, the prominent edges have strong magnitudes. The WNNM operator should be applied in the DPRT domain for effective denoising in the point singularity region. Otherwise standard WNNM operator in spatial domain is applied. This strategy can reduce the effect of the "wrap around" while improving the effectiveness of the WNNM denoising approach around the singularities. Note that when the noise variance is large, the DPRT coefficient tend to accumulate the noise due to the summation effect as illustrated in Fig. 4 (middle). As in some denoising algorithms [3, 6], we perform first-pass denoising as part of the pre-filtering. Its role is to provide a good decomposition in the next stage of the denoising and selecting the similar patches within the group. Following [6], we use BM3D [3] but apply it only in the first iteration. As shown in Fig. 4(right), edges can be accurately detected when the pre-filtered image is used. The detail algorithm of the improved WNNM algorithm is shown in algorithm 1.

Fig. 4. The 10 test images used for evaluation of the competing denoising algorithms

Algorithm 1

***Inputs*:** Noisy image F^n
***Output*:** Denoised image F

```
Initialize F̂ = F^n, F̈ is the pre-filtered image obtained using BM3D
For k = 1:K do
    If k == 1
        Find similar patch group based on pre-filtered image, F̈
    Else
        Find similar patch group based on F̂
    End If
    For each patch in do
        Apply WNNM operator in DPRT domain as in (6), (7), and (10)
    End For
    Aggregate to form the clean image F̂
End For
```

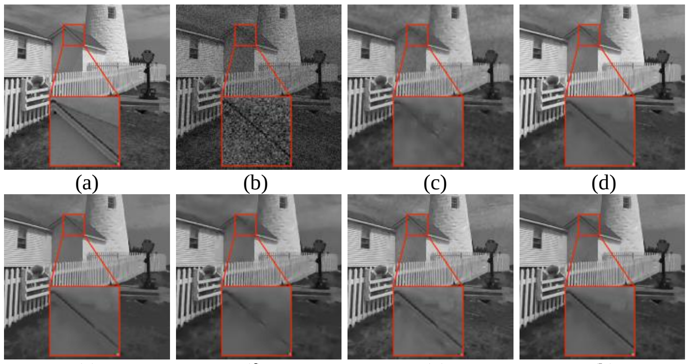

(a) (b) (c) (d)
(e) (f) (g) (h)

Fig. 5. (a). Original image; (b) the noisy image ($\sigma_n = 40$); and the results of by various denoising methods: (c) K-SVD, (d) BM3D, (e) WNNM, (f) MSEPLL, (g) GSRC, (h) Proposed method.

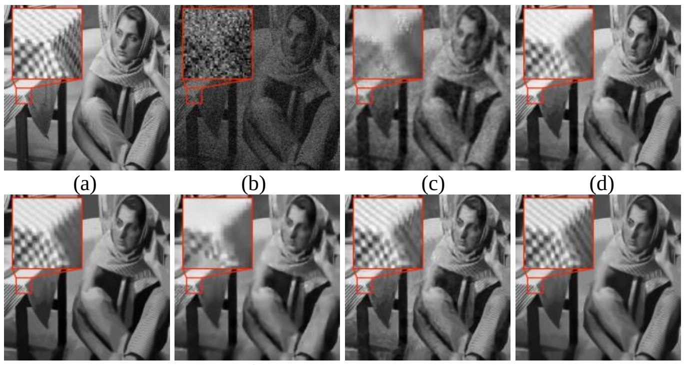

(a) (b) (c) (d)
(e) (f) (g) (h)

Fig. 6. (a). Original image; (b) the noisy image ($\sigma_n = 70$); and the results of by various denoising methods: (c) K-SVD, (d) BM3D, (e) WNNM, (f) MSEPLL, (g) GSRC, (h) Proposed method.

Table 1. PSNR (dB) comparison of competing denoising methods on 10 test images.

Images	$\sigma_n = 10$						$\sigma_n = 40$						$\sigma_n = 70$					
	K-SVD	BM3D	WNNM	MSEPLL	GSRC	Proposed	K-SVD	BM3D	WNNM	MSEPLL	GSRC	Proposed	K-SVD	BM3D	WNNM	MSEPLL	GSRC	Proposed
Lena	35.43	31.71	35.99	35.65	35.85	**36.02**	28.69	28.49	29.96	29.87	29.74	**30.10**	25.22	26.59	26.75	26.51	26.94	**27.08**
Peppers	34.81	24.79	35.06	34.91	34.99	**35.07**	28.55	23.97	29.68	29.65	29.55	**29.83**	24.37	23.25	26.14	25.92	26.23	**26.28**
Boat	33.68	33.92	34.07	33.68	33.92	**34.09**	26.75	27.67	27.75	27.60	27.58	**27.84**	23.33	24.78	24.55	24.45	24.74	**24.82**
Flintstones	32.18	32.44	**32.60**	32.21	32.39	32.59	24.69	25.88	26.22	25.51	26.06	**26.25**	20.25	22.17	21.99	21.50	**22.57**	22.19
Barbara	34.29	31.93	35.45	33.70	34.96	**35.49**	26.33	27.25	28.57	26.11	28.12	**28.65**	22.25	24.69	24.91	22.64	25.06	**25.36**
Light house	32.67	32.84	**33.19**	32.79	32.97	33.16	26.13	27.12	27.27	26.60	27.04	**27.40**	22.54	24.86	24.91	23.77	24.82	**25.07**
Monarch	35.54	32.58	36.71	36.18	36.00	**36.73**	28.20	27.88	29.41	29.10	28.72	**29.45**	23.87	25.38	25.41	25.26	25.53	**25.57**
Plane	35.65	23.07	36.11	35.84	35.90	**36.12**	28.18	22.32	29.47	29.31	29.02	**29.51**	24.34	21.72	26.55	26.32	26.49	**26.66**
Hill	33.40	27.63	**33.79**	33.51	33.70	33.78	27.09	25.50	27.97	27.87	27.89	**28.06**	24.53	24.44	25.22	25.06	25.45	**25.52**
House	35.81	28.24	36.97	35.78	36.74	**37.04**	29.12	26.64	31.17	30.46	30.30	**31.24**	24.96	25.46	28.02	27.32	27.53	**28.09**
Average	34.18	30.10	**34.78**	34.27	34.52	**34.78**	27.18	26.23	28.48	27.96	28.19	**28.57**	23.41	24.21	25.16	24.60	25.32	**25.39**

IV. Experimental Results and Comparison

A series of experiments were performed to evaluate the accuracy the proposed image denoising. In this experiment, we compare the proposed approach with several state-of-the-art denoising methods, including, K-SVD[5], BM3D[3], multi-scale expected patch log likelihood (MS-EPLL)[10], WNNM[7], and GSRC [6]. Except K-SVD, all comparing method exploit the image non-local similarity.

The parameter setting of the proposed method is similar to the conventional WNNM. The searching window is set to 30×30 pixels and iterative regularization is fixed at $\delta = 0.01$. The other parameters are set according to the noise level. When the noise level is high, the slightly bigger patches are chosen and the proposed algorithm run with more iterations. Since DPRT can work only with prime case, the patch size is set to be 7×7 and 11×11 for $\sigma_n \leq 60$ and $\sigma_n > 60$ respectively. The number of iteration K is set to 10, 12, 10, and 14 for $\sigma_n \leq 20$, $20 < \sigma_n \leq 40$, $40 < \sigma_n \leq 60$, and $\sigma_n > 60$. The number of selected non-local similar patches is to 70, 90, 110, and 140 respectively for these noise levels.

All the competing denoising approaches are evaluated on 10 test images as shown in Fig. 4. The first 9 images are of size 512×512 and the last image (house) is of size 256×256. We added Gaussian white noise to the original images to generate the noisy observation with $\sigma_n = 10$, $\sigma_n = 40$, and $\sigma_n = 70$. The simulation results of the comparing methods in term of peak signal-to-noise ratio (PSNR) can be seen in table I. It can be seen that the proposed algorithm outperformed most of the competing methods. Compare to K-SVD, BM3D, WNNM, MSEPLL, and GSRC, it can improve the denoising performance on average by 0.6-2.13dB, 1.19-4.68dB, 0.01-0.24dB, 0.51-0.79dB, and 0.08-0.37dB respectively. The visual comparison for the noise level 40 and 70 between the comparing methods are shown in Fig. 5 and Fig. 6. As shown the Fig. 5, i.e., the strong edge of the roof and Fig. 6, i.e., the texture of the table cloth, the sharp edges can be preserved well in the proposed algorithm outperforming the other denoising method while still maintaining the denoising result of the non-edge area similar to the conventional WNNM denoising. These findings show that DPRT can improve the strong edges even in the present of severe artifacts due to noise.

V. Conclusion

In this research, we improve the conventional WNNM operator for image denoising. With a careful examination of the statistic of DPRT coefficient, we can decomposed the image into two parts, the sharp/strong edges area and the non-edges area. To improve the performance of the denoised image in the sharp edges area, the WNNM operator is performed in DPRT domain which generate the prominent point singularities for sharp edges. Experimental results using the standard test images have demonstrated the effectiveness of the proposed method for denoising the sharp edges. It also outperforms many state-of-the-art denoising methods such as BM3D, MSEPLL, and GSRC in terms of PSNR.

Acknowledgment

The research work described in this paper is fully supported by the Hong Kong Polytechnic University under research grant G-YBK8.

References

[1] P. Chatterjee and P. Milanfar, "Is Denoising Dead?," *IEEE Transactions on Image Processing,* vol. 19, no. 4, pp. 895-911, 2010.

[2] A. Buades, B. Coll, and J. M. Morel, "A non-local algorithm for image denoising," in *2005 IEEE Computer Society Conference on Computer Vision and Pattern Recognition (CVPR'05)*, 2005, vol. 2, pp. 60-65 vol. 2.

[3] K. Dabov, A. Foi, V. Katkovnik, and K. Egiazarian, "Image Denoising by Sparse 3-D Transform-Domain Collaborative Filtering," *IEEE Trans. Image Process.,* vol. 16, no. 8, pp. 2080-2095, 2007.

[4] M. Aharon, M. Elad, and A. Bruckstein, "K-SVD: An Algorithm for Designing Overcomplete Dictionaries for Sparse Representation," *IEEE Trans. Signal Process.,* vol. 54, no. 11, pp. 4311-4322, 2006.

[5] M. Elad and M. Aharon, "Image Denoising Via Sparse and Redundant Representations Over Learned Dictionaries," *IEEE Trans. Image Process.,* vol. 15, no. 12, pp. 3736-3745, 2006.

[6] Z. Zha *et al.*, "Image denoising via group sparsity residual constraint," in *2017 IEEE International Conference on Acoustics, Speech and Signal Processing (ICASSP)*, 2017, pp. 1787-1791.

[7] S. Gu, Q. Xie, D. Meng, W. Zuo, X. Feng, and L. Zhang, "Weighted Nuclear Norm Minimization and Its Applications to Low Level Vision," *International Journal of Computer Vision,* vol. 121, no. 2, pp. 183-208, 2017/01/01 2017.

[8] Y.-X. Liu, Y.-H. Peng, and W.-C. Siu, "Energy-based adaptive transform scheme in the DPRT domain and its application to image denoising," *Signal Processing,* vol. 89, no. 1, pp. 31-44, 2009/01/01/ 2009.

[9] D. Weisheng, S. Guangming, and L. Xin, "Nonlocal Image Restoration With Bilateral Variance Estimation: A Low-Rank Approach," *IEEE Trans. Image Process.,* vol. 22, no. 2, pp. 700-711, 2013.

[10] V. Papyan and M. Elad, "Multi-Scale Patch-Based Image Restoration," *IEEE Trans. Image Process.,* vol. 25, no. 1, pp. 249-261, 2016.